1962

A study of the stress distribution around circular openings using multilayered photoelastic material

Donald Frank Haber

Recommended Citation

Haber, Donald Frank, "A study of the stress distribution around circular openings using multilayered photoelastic material" (1962). *Masters Theses*. 2727.
https://scholarsmine.mst.edu/masters_theses/2727

A STUDY OF THE STRESS DISTRIBUTION AROUND CIRCULAR OPENINGS USING MULTILAYERED PHOTOELASTIC MATERIAL

BY

DONALD HABER

A

THESIS

submitted to the faculty of the

SCHOOL OF MINES AND METALLURGY OF THE UNIVERSITY OF MISSOURI

in partial fulfillment of the work required for the

Degree of

MASTER OF SCIENCE, MINING ENGINEERING

Rolla, Missouri

1962

Approved by

George B Clark (advisor) John B. Heagler Jr.

Ralph E. Lee R. F. Dawson

ACKNOWLEDGMENT

The writer wishes to thank Professor G. B. Clark, Associate Director of the Research Laboratories, University of Missouri School of Mines and Metallurgy, for his advice and help. He is also grateful to Professor R. F. Davidson, chairman of the Mechanics Department for his advice and to R. A. Travis, Mining Research Branch, U. S. Bureau of Mines, Rolla, Missouri, for his help in obtaining the necessary equipment and chemicals.

TABLE OF CONTENTS

LIST OF FIGURES

LIST OF TABLES

INTRODUCTION

Stress analysis as applied to mine openings ranges from the completely empirical to the completely theoretical. However, it is only through the ultimate utilization of the two methods that a guide to the interpretation of mine stress phenomenon may be obtained. The bridge between the two approaches lies in the field of model study. Specifically, this is an investigation into determining the feasibility of using multilayered photoelastic materials in models such that a more exact approximation of the underground stress distribution around mine openings can be made.

The two major objectives in this study for determining the feasibility of using multilayered photoelastic material were as follows:

1) To develop a material which can be used as a photoelastic material and easily cast into sheets having different physical constants.

2) To apply this material to a solution of a specific problem. That is the analysis of the stress distribution around a circular opening occurring in two layers of material with different moduli of elasticity.

The importance of the stress distribution around mine openings can be summed up into two parts:

1) The design of the mine opening could lessen the stress concentration, thereby, providing a safer environment for the mine workers;

2) The amount of materials and supports can be optimized, thus increasing the percentage recovery of ore.

Previous Work

Probably the first investigation into the stresses in a three dimensional medium came from Boussinesq(1), who used the theory of elasticity to solve for the stress distribution in a semi-infinite, three dimensional, elastic medium due to the application of a point load at the boundary. Flamant(2) solved the Boussinesq problem, for a point load on a semi-infinite two dimensional plate. J. H. Michell(3) solved the stress distribution problem in an elastic medium for a finite uniform load on a semi-infinite plate. Kirsch, Greenspan, Koloff and Englis(4) all used applied elasticity to solve for the stress distribution around various shaped openings in semi-infinite plates.

The first use of photoelasticity as applied to the stress in an earth mass could be attributed to Coker and Filon(5). They compared the stresses found in a semi-infinite plate loaded with a finite distributed load using photoelasticity, with the values of stress found using Michell's mathematical solution. Bucky and Sinclair(6) did some of the first work using photoelasticity applied directly to mining problems. They used a photoelastic method to test the effects of overburden loading on mine pillars, and also under the pillars. The load was applied to the pillars by a centrifuge in order to simulate the action of gravity. They also investigated the effects of tunnels near mine pillars on the stress distribution in the pillars using the photoelastic technique.

Panek(7) investigated the stresses induced by horizontal openings subjected to various states initial of stress. Simple geometric openings in homogeneous mediums were studied first and solutions for the stress distribution about these openings were found by the methods of methematical theory of elasticity. These results were compared with solutions obtained by photoelastic methods for single and multiple openings. Panek also showed that if the depth from the earth surface to the top of the opening in a homogeneous medium is more than twice the long cross-sectional dimension of the openings, the tangential stress on the boundary is for practical purposes unaffected by the boundry. Under conditions of hydrostatic pressure, an opening of circular cross-section will induce the smallest critical stress. Finally Panek listed the primary factors governing the magnitudes of the critical stresses as: (1) the length to width ratio of the cross-sectional dimensions of the opening; (2) the pillar width; (3) the ratio of vertical to the lateral initial earth pressure(7).

Duvall(8) used a photoelastic technique and ran tests very similar to Penek, although he used both hydrostatic and uni-directional loading. Duvall's results were in agreement with Panek although more specific in nature.

Van Poollen (9) used the photoelastic analogy to base his argument for horizontal supports in mine openings. A photoelastic model of rectangular opening in a homogeneous medium was constructed and tested. Assuming failure strengths for rocks in compression, tension and shear, a failure zone could be established. If the rocks in this failure zone are allowed to cave, the span of the roof will be increased, thus causing a larger area to be in tension and the possibility of more rocks failing in tension. If horizontal supports are used, Van Poollen contends, that the rock in the failure zone can be prevented from caving, thereby keeping the roof span constant.

More recently Moye (10) reported a complete investigation of Engineering Geology and Rock Mechanics in an underground power station in Australia. Photoelasticity was used in conjunction with stresses measured by the use of flatjack. The flatjack method gave a good estimate of the actual stresses present. Since the photoelastic method gives the stresses due only to overburn weight, the tectonic or residual stresses could be calculated from the difference in stresses found by these two methods. Moye used gelatin as his photoelastic medium in order to simulate overburden weight.

E. L. Potts (11) examined the stress distribution around single underground roadways of different shapes using photoelasticity. His results again agreed with Duvall (8) and Panek (7). Another attack was used to solve the problem of the stress distribution found by boring holes in a coal pillar. The coal seam and adjacent rock were represented by two photoelastic materials with different physical constants. These physical constants were arranged such that the ratio of the modulus of elasticity of adjacent rock to the coal seam was the same as the ratio of the modulus of elasticity of two photoelastic materials. The final result was the determination of the number of holes, their spacing from each other and the pillar edge, without materially reducing the strength of the pillar.

Along with Potts' work, J. Dixon(12) ran a similar series of tests using rectangular auger openings instead of circular openings. This was done because the results of the previous investigations by Potts(11) indicated that the coal tensile strength was less than the value found by investigation and the coal would fail at the top and bottom of the opening enlarging the opening into a rectangular shape.

Justification of Photoelastic Model Studies

In most of the photoelastic literature referenced in this study, the exception being the work done by Potts and Dixon, two very basic assumptions had to be made. One, that the earth surrounding the opening is homogeneous. Two, that the medium can be considered isotropic (that is, the constants describing the physical behavior of the medium are constant in all directions and do not vary from point to point.) Various investigators (7, 8, 10,12, 13, 14) have attempted to justify this assumption with the general consensus being that although the earth is far from the homogeneous and isotropic medium assumed, the application of photoelastic model study to mine problems does indicate:

1) A comparison of stress between one structure and another
2) A method of attack by which mine stress problems can be investigated
3) The regions of probable distress
4) A better understanding of which physical tests of rock would give the most information to the physical properties which could lead to the ultimate solution.

With the assumption that all the earth is made of a layered homogeneous materials, instead of being entirely homogeneous, a closer approximation of the actual stress distribution around openings in the earth can be made.

PHOTOELASTIC MODEL MATERIAL

The basic requirements of the material used in this research can be stated briefly as follows: It must be transparent, birefringent, and elastic. It must be relatively easy to manufacture, machine, and handle, and have a high stress optic sensitivity. It also must be easily cast into layers with different modulus of elasticity.

Gelatin

A survey of the existing literature was conducted in an attempt to find a photoelastic material which would satisfy these requirements. Gelatin meets most of the requirements listed. It was tried in the initial studies of this research. However, gelatin has a very detimental time-edge effect, poor machinability, high strain fringe value, i.e., strain necessary to produce one fringe in a model of unit thickness, and finally is very difficult to cast into layers which have different moduli of elasticity. However, gelatin as a photoelastic material, is extremely sensitive to stress, i.e., a very small stress (.0725 psi/fringe/in for shear stress in thickness) will produce one fringe. This enables one to use gelatin in studies involving body forces. Several early investigators (16, 17, 18, 19, 20, 21, 22, 23, 24) used gelatin in photoelastic studies for the stress distribution around dams, tunnels, and foundations. In this study, the fact that gelatin was extremely hard to handle and the detrimental time effect overbalanced its advantage of sensitivity.

Epoxy Resin

The survey of existing literature also pointed up the increased use of epoxy resins as a photoelastic materials. Several investigators had made use of a clear epoxy resin in photoelasticity and reported good results, (24, 25, 26, 27, 28). From these reports, Araldite 502, a liquid organic resin was chosen as the photoelastic material. This resin when combined with a suitable hardener and other solvents will cure to a solid material with different physical and optical properties.

History and Structure of Epoxy Resins

Epoxy resins are the newest of the major industrial plastics. They were first synthesized by Pierre Castan in Switzerland and S.O. Greenlee in the United States late in the 1930's. (29) Epoxy resins are thermosetting materials, that is, when converted by a curing agent, the resins become hard in fusible systems. The system may be visualized as a network crosslinked in all three dimensions. In a plane it might appear as shown. The epoxy molecules are represented diagramatically by a horizontal line and the crosslinking between the system of molecules is shown by the vertical line.

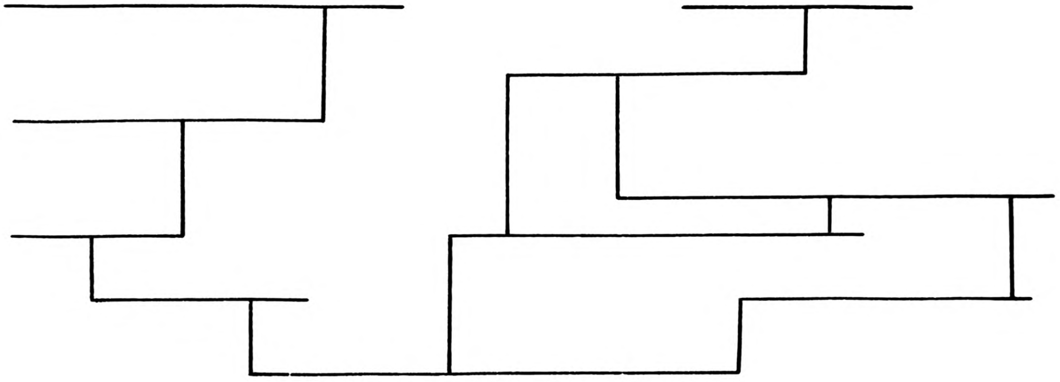

Thus the movement of a molecule in any direction is opposed by the crosslinking arrangement. This crosslinking gives the epoxy system much more strength than the typical thermoplastic plastic which does not have crosslinking.

The thermosetting epoxy resins possess a number of unusually valuable properties which could be applied to use in the formation of adhesives, sealing liquids, cold solders, casting and coating. The more important of these properties are:

1) Versatility: Numerous curing agents for the epoxies are available, and the epoxies could be used with a wide variety of modifiers. Therefore, the properties of the cured epoxy-resin system can be designed to meet widely different specifications.
2) Good handling characteristics: Most epoxy systems can be used and worked at room temperature. Before the curing agent is mixed into the system, the resins have indefinite shelf life.
3) High adhesive properties: Epoxy resins have high adhesive strengths arising from the polarity of the atomic groups present in the initial resin chain, and in the cured system. The polarity of these groups serves to create electro-magnetic bonding forces between the epoxy molecule and the adjacent surface.

Casting the Epoxy Resin

Since Epoxy Resin was first developed as an adhesive, a method had to be devised which would allow the epoxy to be cast into a sheet of uniform thickness and be separated from the mold itself, without causing any damage to the sheet or mold. After considerable research into different mold release agents, it was found that lucite plastic could be used without any release agents whatsoever. Figure No. 1 on page 11 shows the actual mold. This mold consisted of two flat plates of Lucite separated by brass ball bearings used as spacers. The brass ball bearing spacers give three point support. The final thickness of the solid sheet did not vary over .005 inches. Tape was used around the sides and bottom of the mold to prevent leakage of the liquid resin.

The resin had to be thoroughly stirred before pouring into the mold. If it was not thoroughly mixed, distortion of the light due to the inhomogeneity of the final material occurred and gave a distorted fringe pattern.

Chemical Composition of the Cured Resin

Since the Epoxy Resin Araldite 502 is liquid at room temperature, a hardening material was used to obtain a solidified product. In this study, a chemical liquid hardener manufactured by the Ciba Chemical Company, Fairlawn, New Jersey, under the trade name of "951" was used. As previously stated the amount of hardening material or hardener used with the liquid resin determines the physical and optical properties obtained in the final product.

A series of tests were run to determine the best hardener to resin ratio which would yield the desired physical requirements. It was found, however, that if Araldite 502 and hardener 951 were

FIGURE 1

Model Casting Apparatus

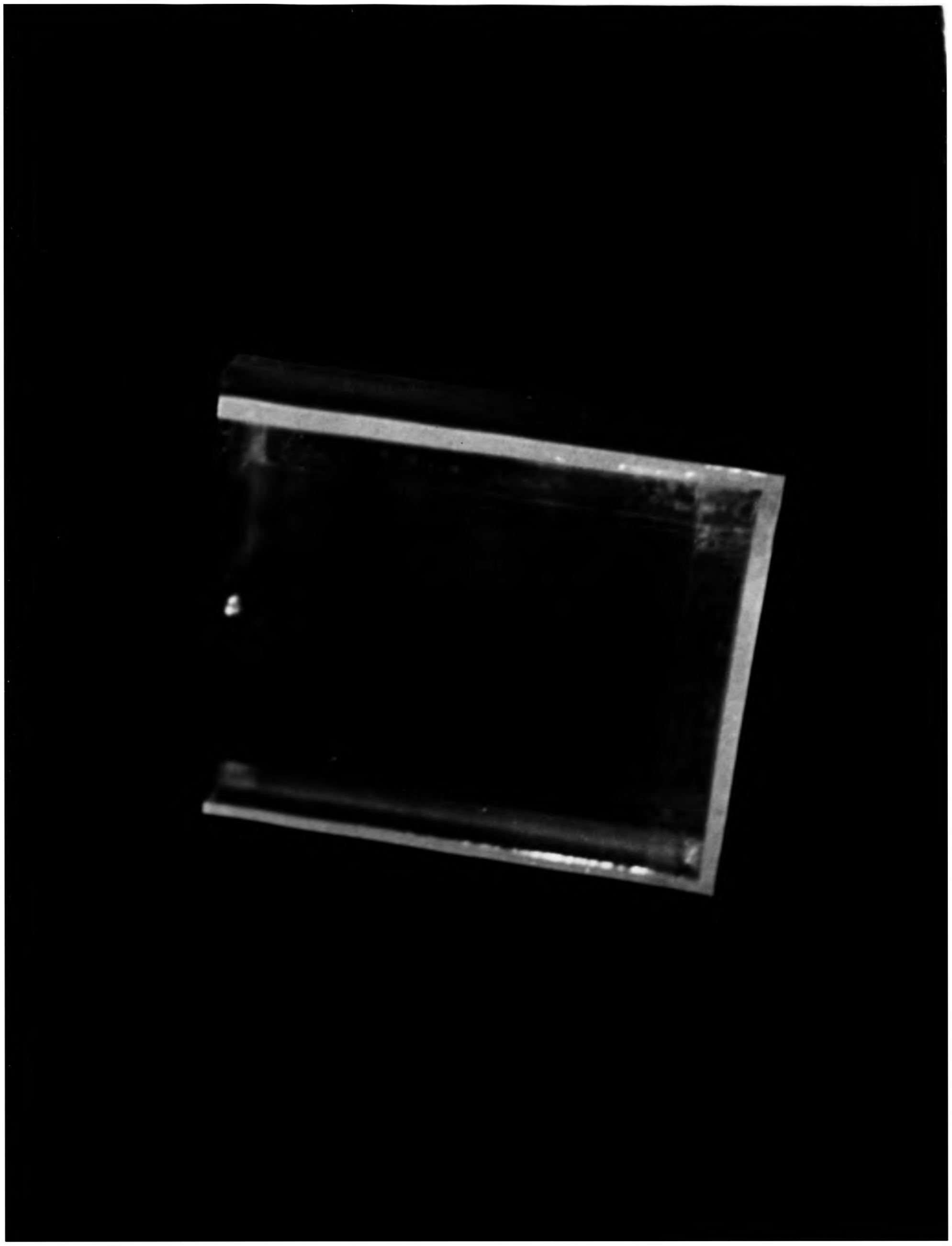

used exclusively, initial or "locked in" stresses were obtained in the cured product. Annealing the cured product or varying the curing temperature did not relieve the "locked in" stresses and other methods had to be found. After trying various chemical plasticisers and organic solvents, two chemicals were found that if used in the proper proportions with the resin and hardener they would relieve the "lock-in" stress and provide a stress-free photoelastic material. These chemicals were cyclohexanol and Dibuty-phthalate. Another series of tests were run to determine what proportions of the chemicals constituents would give the desired physical properties without any residual stresses appearing in the final product.

Table 1 on page 13 gives the results of the two series of tests in regard to what proportions were used and how this affected the properties of the cured resin.

TABLE NO. 1

Experimental Results of Modulus of Elasticity and Material Fringe Value for Composition of Epoxy Resin

Run No.	% 502	% 951	% Cyclo.	% Dibutyl	E psi	f psi	Comments
1	36.8	3.2	20.0	40.0	----	----	weak
2	36.8	3.2	30.0	30.0	----	----	cracks
3	36.8	3.2	40.0	20.0	----	----	cracks
4	46.0	4.0	10.0	40.0	----	----	cracks
5	46.0	4.0	20.0	30.0	70	----	cracks
6	46.0	4.0	30.0	20.0	----	----	cracks
7	54.0	4.7	14.3	27.0	----	----	creep
8	55.2	4.8	20.0	20.0	----	----	weak
9	55.2	4.8	10.0	30.0	----	----	weak
10	56.0	6.5	23.4	14.0	300	1.36	
11	56.0	6.5	23.4	14.0	375	1.04	see ref.27
12	56.0	6.5	23.4	14.0	325	1.38	
13	56.0	6.5	23.4	14.0	305	1.40	
14	57.2	4.7	23.7	14.3	123	1.08	

TABLE NO. 1 (Continued From Page 13)

Run No.	% 502	% 951	% Cyclo.	% Dibutyl	E psi	f psi	Comments
15	57.2	4.7	23.7	14.3	150	1.14	
16	61.5	5.4	33.5	0	18,300	24.20	
17	63.0	5.5	24.6	6.9	361	----	creep
18	64.4	5.6	15.0	15.0	----	----	creep
19	64.4	5.6	25.0	7.0	----	----	creep
20	71.0	5.7	9.5	14.3	60	1.40	creep
21	72.0	8.0	0.0	20.0	993	2.44	see ref.28
22	73.6	6.4	10.0	10.0	2,000	----	creep
23	76.0	6.2	7.0	11.5	40	1.50	
24	78.0	6.2	7.9	7.9	43	1.50	
25	88.0	12.0	0.0	0.0	----	68.00	initial stresses
26	90.0	10.0	0.0	0.0	450000	----	see ref. 30
27	90.0	10.0	0.0	0.0	386000	74.00	see ref. 26
28	91.0	9.0	0.0	0.0	----	50.50	initial stresses
29	94.0	6.0	0.0	0.0	----	1.29	initial stresses

MODEL TESTING OF EPOXY RESINS

The cured epoxy resins differed in Engineering properties due to the different chemical constituents. Before the actual model tests were run, the Modulus of Elasticity and the Material Fringe Value were determined.

Determination of Modulus of Elasticity

The modulus of elasticity of the cured resin was obtained by measuring the deflection of a simply supported beam under a concentrated load as shown by figure 2 on page 16. The equation for deflection of a simply supported beam under a concentrated load is given as:

$$\Delta = \frac{PL^3}{48\ EI} \quad \text{where}$$

P = Concentrated load

E = Modulus of elasticity

I = Moment of inertia of the area about the centroidal axis

L = Length of span

Δ = Deflection of the center of the beam

Solving for E

$$E = \frac{PL^3}{48\,\Delta I}$$

Table 1 on page 13 gives the results of these tests.

FIGURE NO. 2

Test for Determination of Modulus of Elasticity "E"

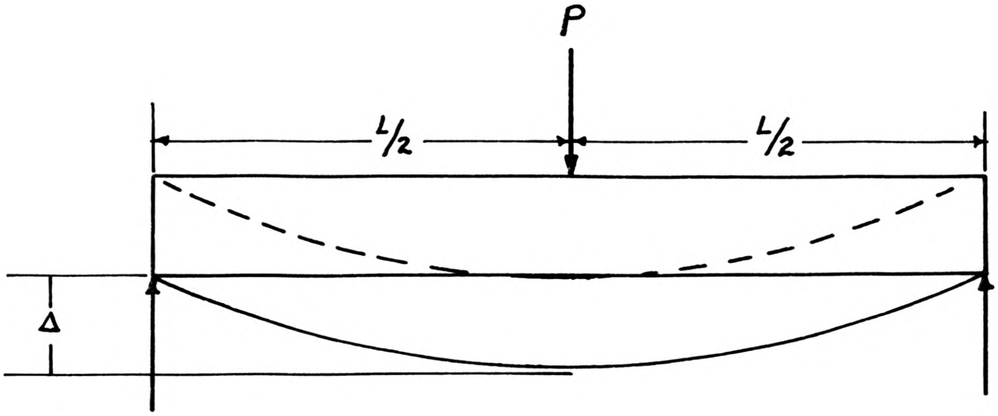

$$\Delta = \frac{PL^3}{48EI}$$

$$E = \frac{PL^3}{48\,\Delta I}$$

Determination of Material Fringe Value

Since a variation of hardener and plasticiser caused the modulus of elasticity of the material to change, it was necessary to test each material to determine the material fringe value (f), i.e., the stress necessary to produce one fringe for inch of thickness of the model. These values are tabulated in table 1 on page 13 for the various proportion of chemicals. In several tests, no value of the material fringe value or modulus of elasticity was obtained. This was caused by three basic difficulties:

1) Strength: When the proportion of 951 hardener to Araldite 502 fell below 6% or the ratio of 502 and 951 to cyclohexanol and dibutylphthalate was less the 60-40, the material was extremely weak and cracked with the application of concentrated loads to its surface. Also, if the cured material was exposed to the air for a period exceeding 24 hours, tension cracks appeared in the material. This phenomenon is shown in figure 3 on page 18.
2) Creep: If the percent of Dibutyl-phthalate is high (approximately 20% by weight), the material exhibits creep, i.e., deformation which continues with time under a constant stress. It has been reported by Durelli, Dally and Riley (5) however, that the final deformation (after a long period of time) is pro-

FIGURE 3

Cured Resin After Four Days

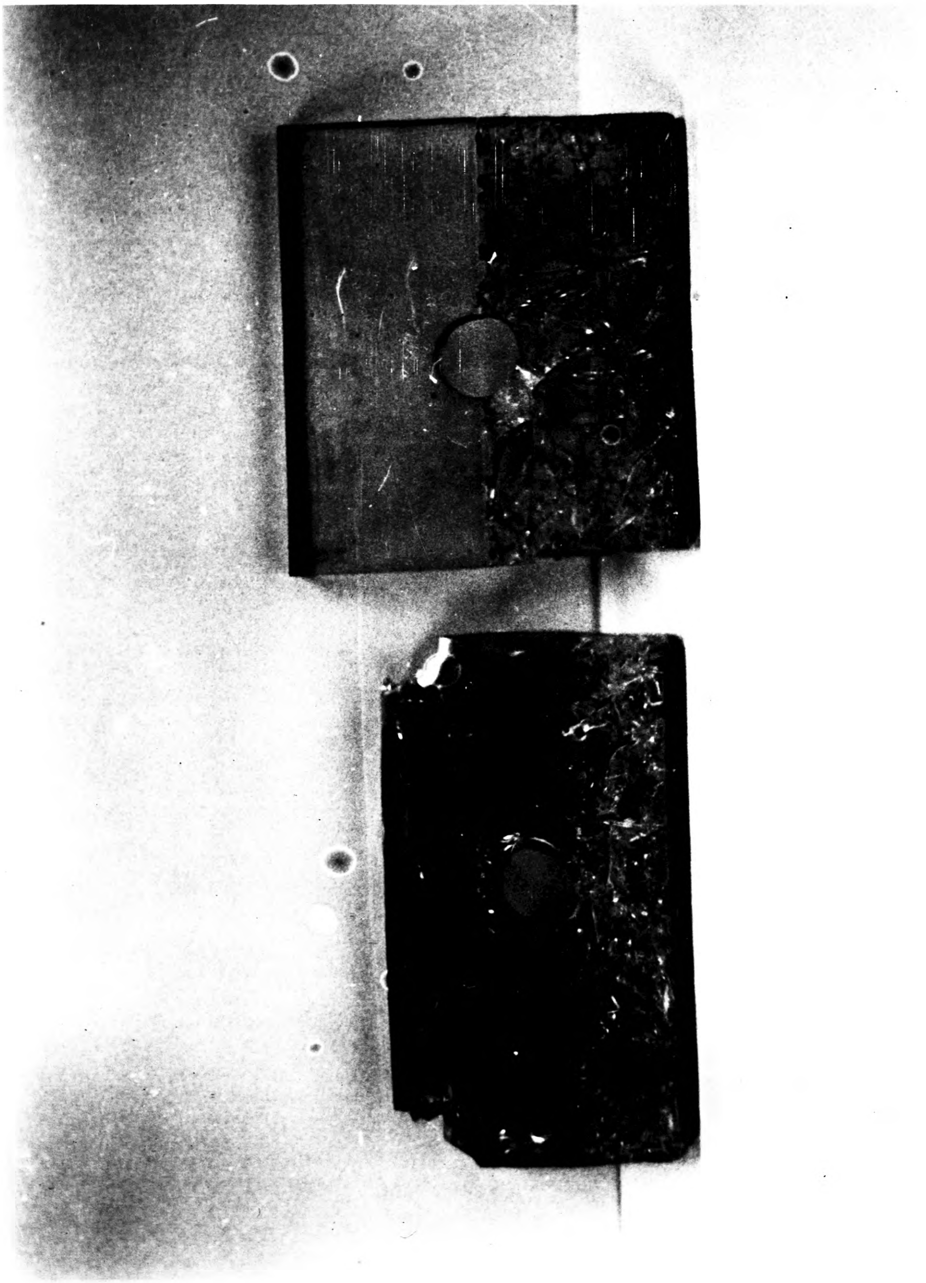

portional to the load applied. Since a more resilient system was desired, these tests for (f) were discontinued.

3) Initial Stresses: As previously stated, if no plasticisers or modifiers were used with the 502-951 system, initial stresses appeared in the cured resin. These initial stresses prevented the test for E and (f) in some cases.

The actual test for the material fringe value consisted of a concentrated load on a semi-infinite plate as shown in figure 4 on page 20. The value for stress on a vertical line of symmetry extending from the point of application can be found from the mathematical theory of elasticity,$^{(8)}$ to be $\sigma_r = \frac{2P}{\pi r}$ where

σ_r is the radial stress

P is the applied load/unit thickness

r is the vertical distance from the applied load to the point directly below the load at which the stress is desired. The actual stress distribution at any point in a semi-infinite medium due to a vertical concentrated load on its surface is given as$^{(8)}$.

$$\sigma_r = \frac{2P \cos \theta}{\pi r}$$

FIGURE 4

Concentrated Load on a Semi-infinite Plate

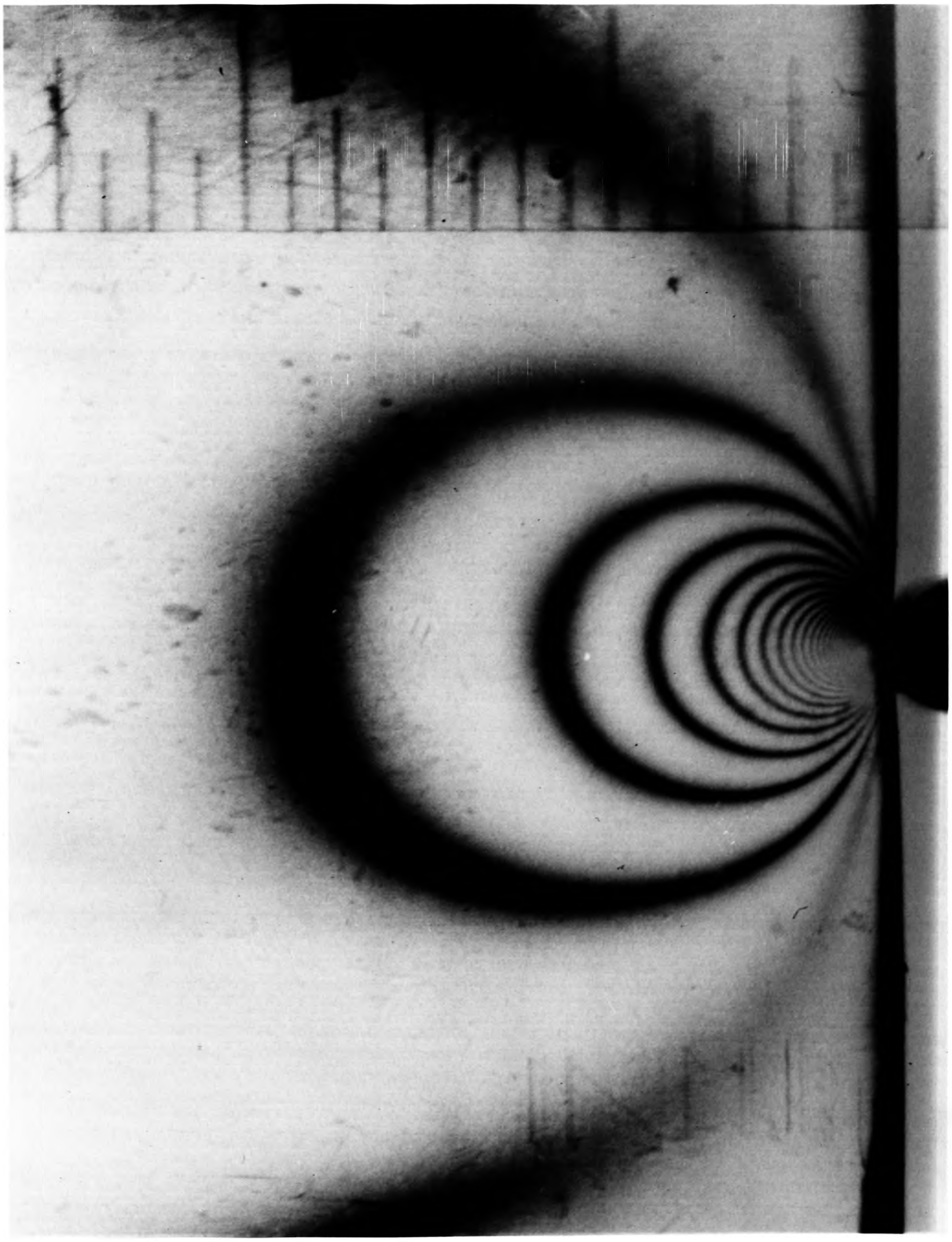

FIGURE NO. 5

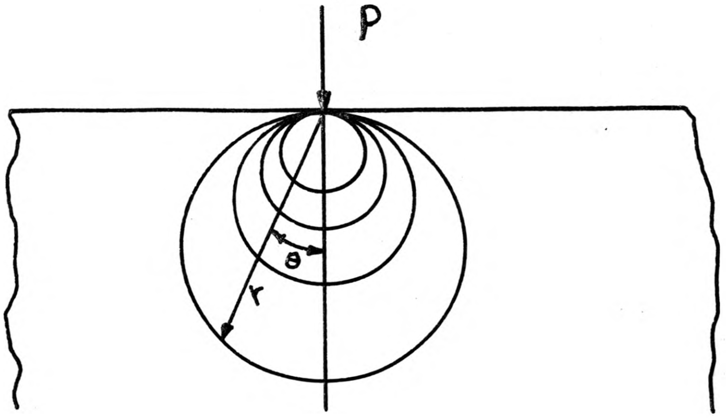

This distribution can be thought of as circular lines of equal radial stress starting from the point of application as shown in figure 5.

In photoelasticity, the fringe order represents the difference between the principal stress ($\sigma_1 - \sigma_2$). The higher the fringe order the larger the difference between principal stresses. This relation between fringe order and difference in principal stress should be linear for an elastic, birefringent material. Figure 4 on page 20 shows the fringe distribution due to a concentrated load on a sheet of cured resin.

As noted in this picture, the similarity between the photoelastic fringe distribution and the exact mathematical solution indicates that the material is elastic and has a fringe distribution which varies with the actual stress in the model. Since on a radial element, the compressive stress σ_r is the only stress present, the difference in principal stress is the stress σ_r. Therefore:

$$\sigma_1 - \sigma_2 = \frac{nf}{t}$$

where n = fringe order

f = material fringe value lb/in^2 for in/fringe

t = thickness of the material

therefore:

$$\sigma_r = \frac{nf}{t} = \frac{2P}{r}$$

(For all points falling on the vertical line thru the concentrated load.)

A plot was made between Log (n) and log (r) and a straight line was obtained. Figure 6 on page 23 shows an example of this. The values for the stress and fringe order at two points (r_1, n_1) and (r_2, n_2) were taken from this graph. The points (r_1, n_1) and (r_2, n_2) were found from the figure 4 on page 20.

$$\text{Since } \sigma_{r_1} = \frac{2P}{\pi r_1} \quad \text{and} \quad \sigma_{r_2} = \frac{2P}{\pi r_2}$$

$$\text{and } \sigma_{r_1} = \frac{n_1 f}{t} \quad \text{and} \quad \sigma_{r_2} = \frac{n_2 f}{t}$$

$$\sigma_{r_1} - \sigma_{r_2} = \frac{n_1 f}{t} - \frac{n_2 f}{t}$$

solving for the material fringe value

$$f = t\left(\frac{\sigma r_1 - \sigma r_2}{n_1 - n_2}\right)$$

All the material fringe values were found by this method approximately 24 hours after the resin had cured. The material fringe value was also found just prior to a test on models. This was done because of the change in this value with time.

FIGURE NO. 6

Graph of Distance from Load vs. Fringe Order

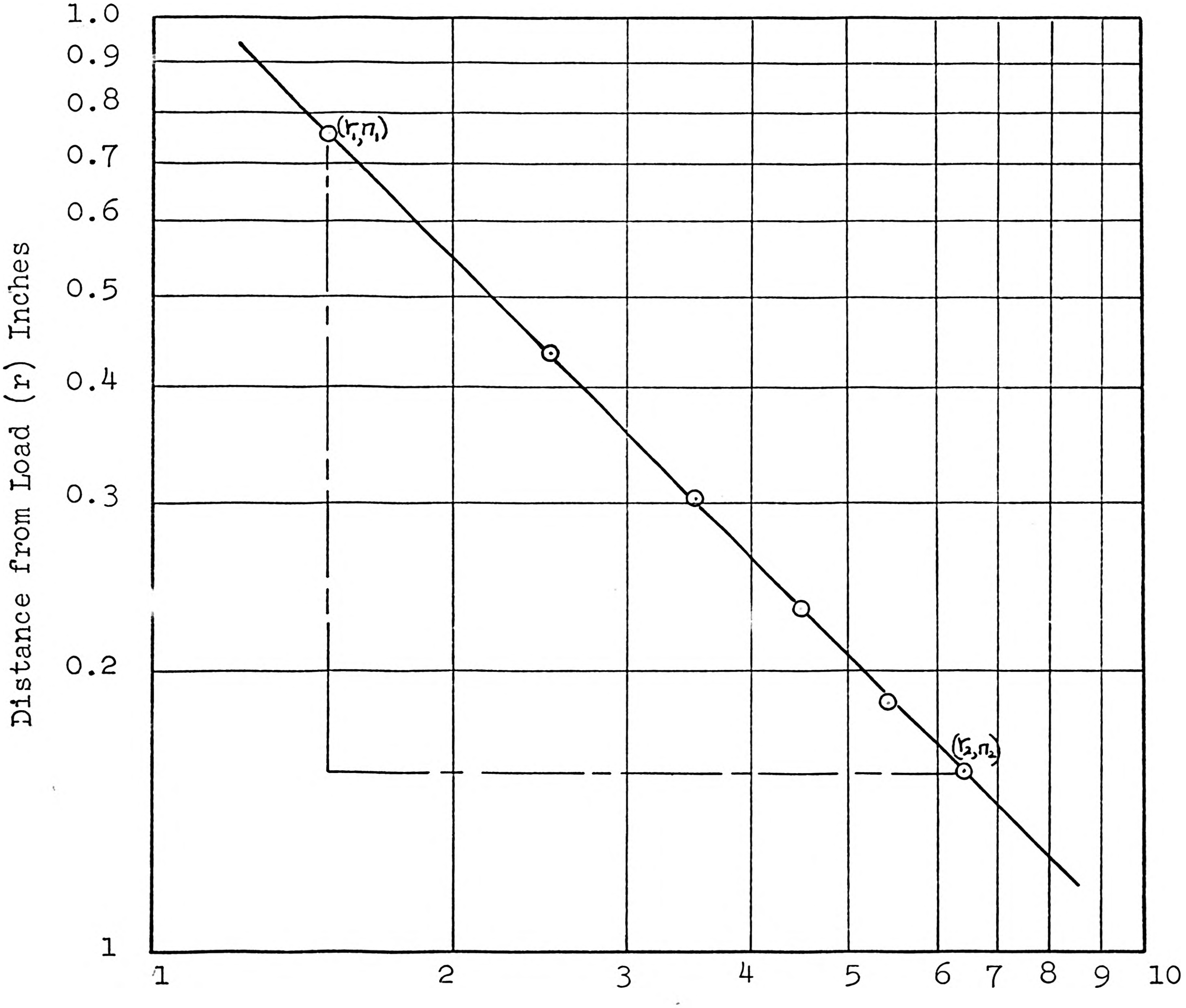

Loading Device

Figure 7 on page 25 shows the loading arrangement for applying a distributed load to a sheet of model material. A very stiff bar of metal was used to apply the distributed load to the top surface of the model. Since friction was set up between the bar and the model, the influence of this friction on the stress-fringe distribution was checked. At any point over one inch from the top surface, the stress had distributed itself according to St. Venant's principal and was not affected by the friction and the elastic constraint at the surface. Loads were applied to the metal bar by means of a lever arm system. The load was applied to a small metal cylinder in the center of the bar.

Machining the Model

Because smooth circular holes were used as the openings in the models, an effective device had to be used to machine the cured resin. Figure 8 on page 26 shows the router which was used in this study. The cured material could easily be machined by this router and the router left no machine stresses. Any other suitable machine shop high speed cutting devices could be used in shaping the material without tearing.

The Optical Setup

Figure 9 on page 27 shows the polariscope used in this study. It is a standard bench polariscope. A white background was used throughout the study because of the superior contrast in the final photographs.

FIGURE 7

Loading Device

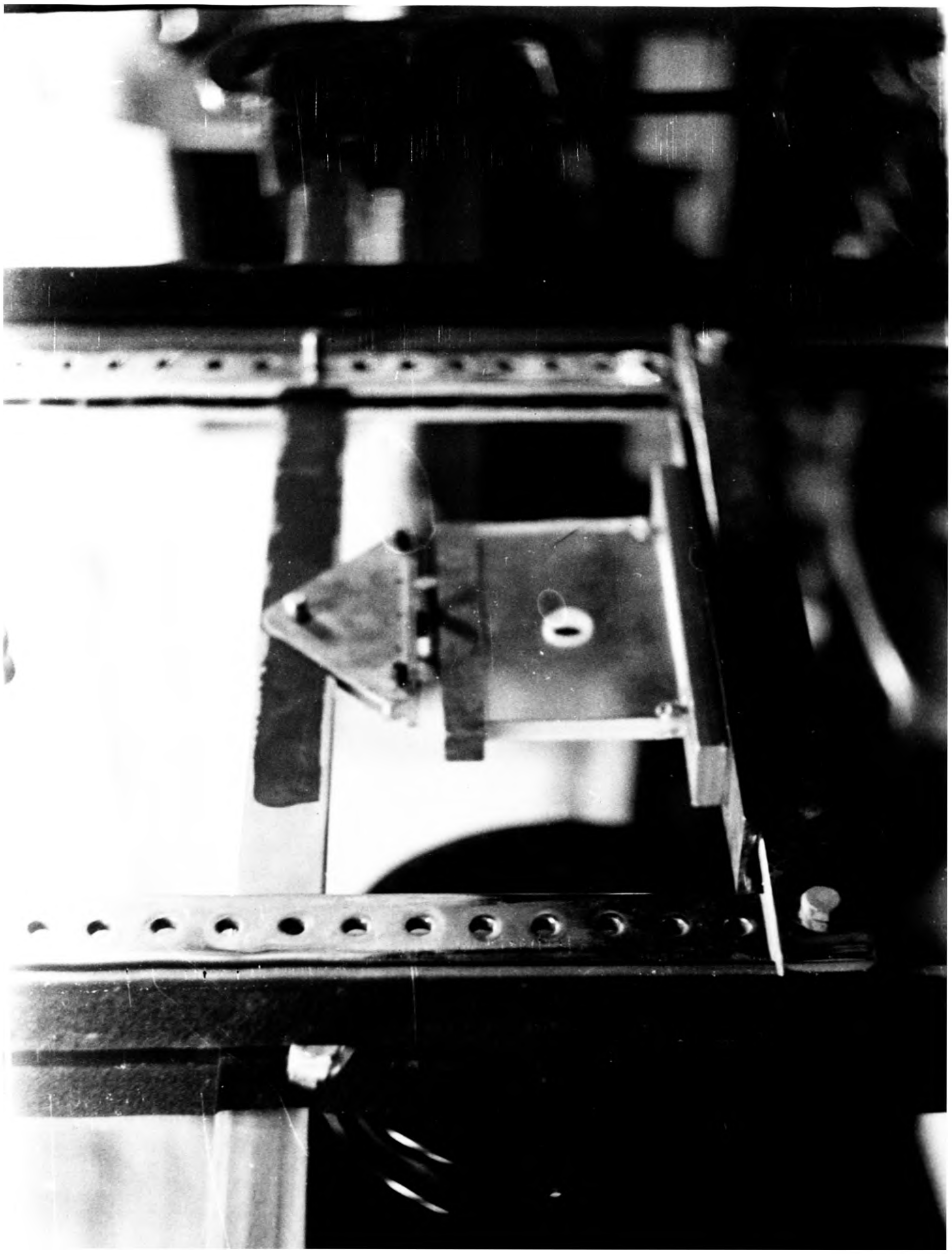

Figure 8

Model Machining Apparatus

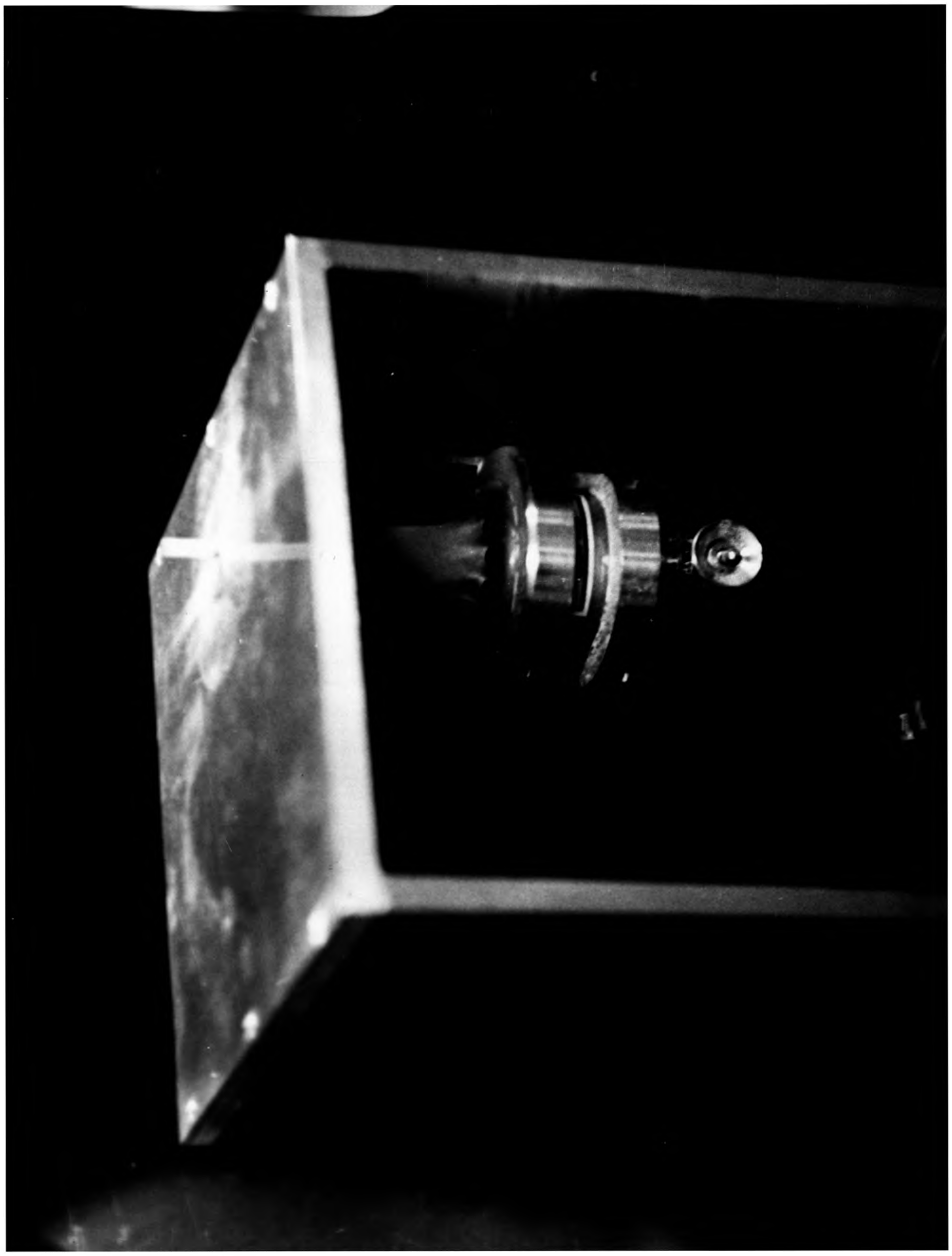

FIGURE 9

Polariscope

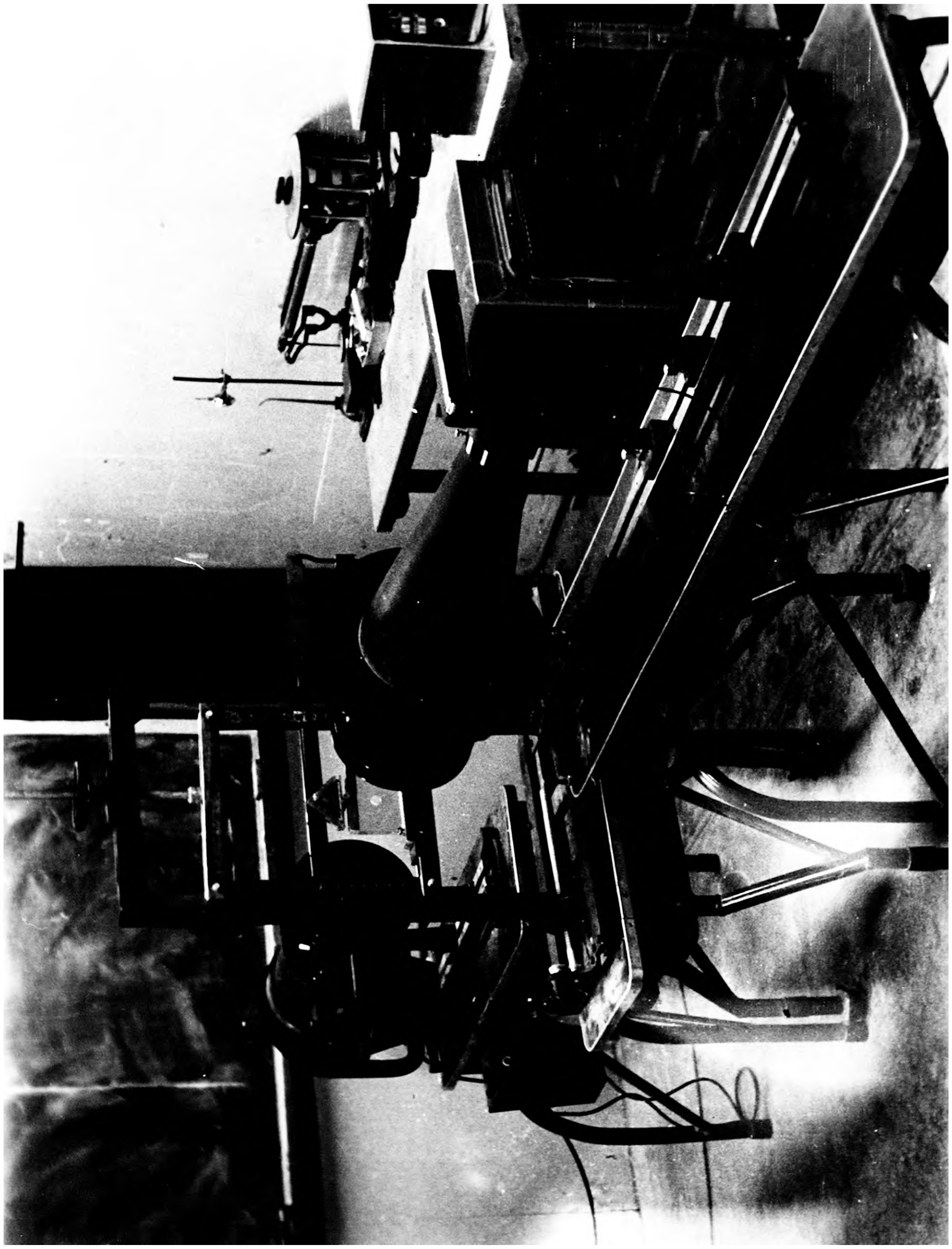

TEST OF A CIRCULAR OPENING IN A HOMOGENEOUS MEDIUM

In order to check the accuracy of the calibration procedure and the loading device, a test was run using a circular opening in a homogeneous semi-infinite sheet subjected to a uniformly distributed load on its boundry. An exact methematical solution is available for this case$^{(8)}$. Figure 10 on page 29 shows a plate subjected to a uniform compression of magnitude S in the x direction. The stress distribution shown in the plate is given by

$$\sigma_r = -\frac{S}{2}\left(1 - \frac{a^2}{r^2}\right) - \frac{S}{2}\left(1 + \frac{3a^4}{r^4} - \frac{4a^2}{r^2}\right) \cos 2\theta$$

$$\sigma_\theta = -\frac{S}{2}\left(1 + \frac{a^2}{r^2}\right) - \frac{S}{2}\left(1 + \frac{3a^4}{r^4}\right) \cos 2\theta$$

$$\tau_{r\theta} = -\frac{S}{2}\left(1 - \frac{3a^4}{r^4} + \frac{2a^2}{r^2}\right) \sin 2\theta$$

where r is the radial distance from the center of the hole

S is the applied load

a is the radius of the hole

θ is the angle between r and the fixed axis x

σ_r is the radial normal stress

σ_θ is the normal stress in the circumferential direction

$\tau_{r\theta}$ is the shearing stress associated with the point r, θ

The stress at the edge of the hole was desired, so (r) was set equal to (a) and

FIGURE NO. 10

A Plate Submitted to a Uniform Compressive Stress (S) in the X-Direction

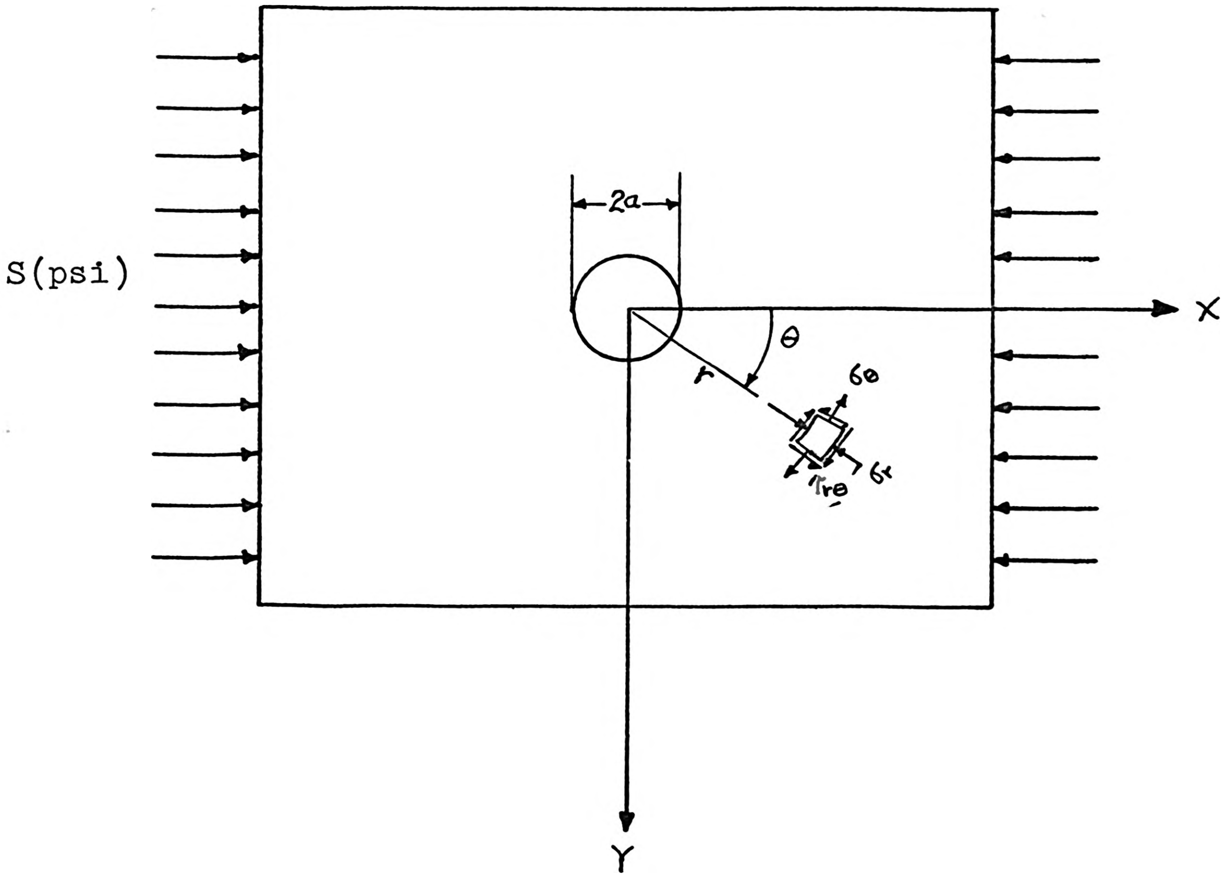

$$\sigma_r = \sigma_{r\theta} = 0$$

and

$$\sigma_\theta = S - 2S \cos 2\theta$$

The stress at $\theta = 0, \pi$ gives

$$\sigma_\theta = -S + 2S\ (+1) = +S$$

and the stress at $\theta = \frac{\pi}{2}, \frac{3\pi}{2}$

$$\sigma_\theta = -S + 2S\ (-1) = -3S$$

This exact solution states that the top and bottom of a circular hole subjected to a uniformly distributed compressive load the stress should be tensile and equal to the applied stress. At the two sides of the hole, the stress should be three times the actual compressive stress applied to the system.

In terms of the actual applied stress, the stress Concentration factor at the two sides of the hole would be 3 and the S.C.F. at the top and bottom would be 1. These stress concentration factors were compared against the ones found using the Epoxy Resin Material.

Figure 11 on page 31 shows the fringe distribution obtained from a test of a uniform applied compressive stress to a circular hole in the cured resin. This stress distribution compares very closely with Frocht's picture of a similar case (9). The material fringe value of the material used was found to be

FIGURE 11

Fringe Distribution Around a Circular Hole in a Homogeneous Medium

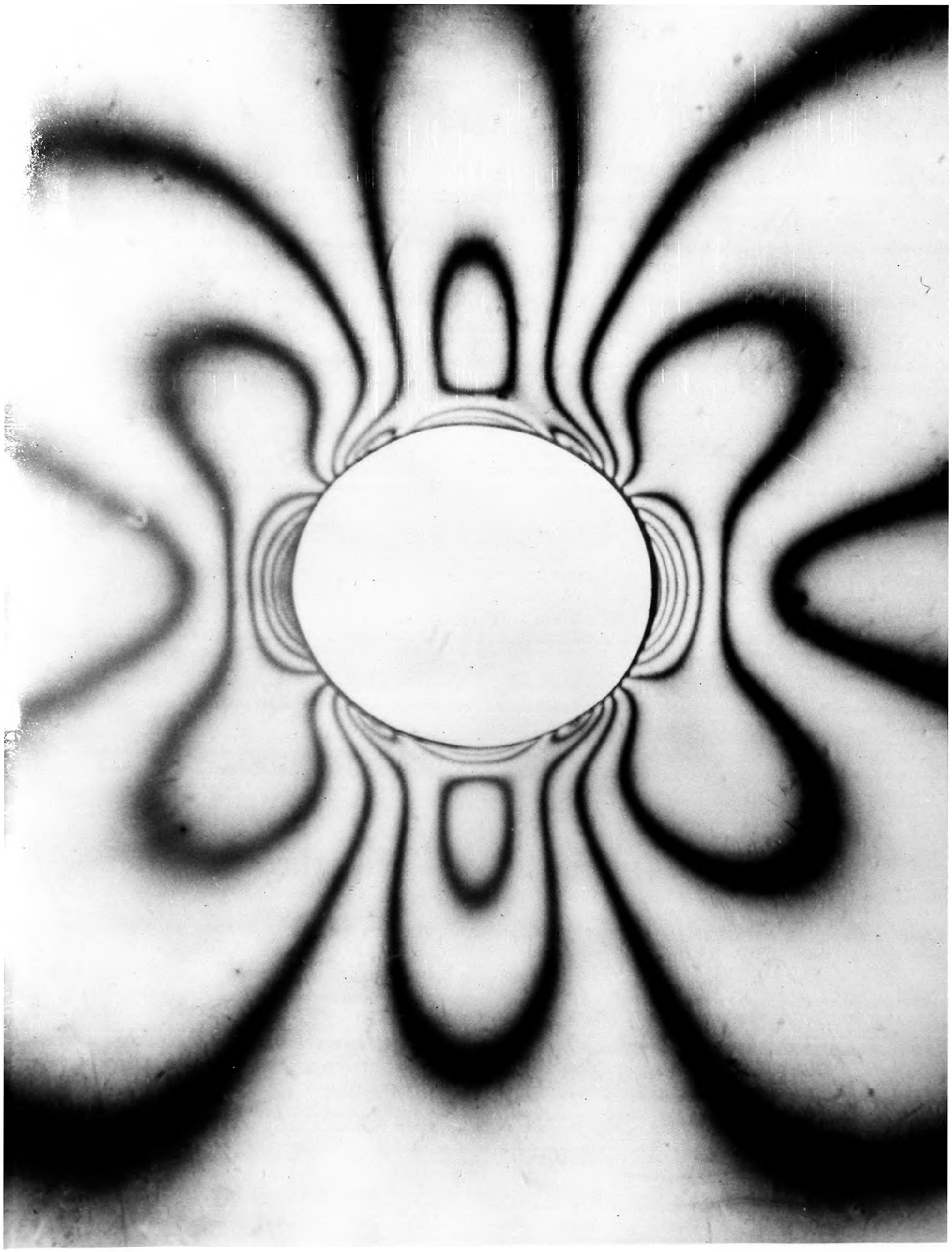

$$f = 1.25 \text{ lb/in}^2 \text{ for in/fringe order}$$

the model fringe value is given as:

$$F = \frac{f}{t}$$

where t is the thickness

Therefore

$$F = 2.55 \text{ lb/in}^2\text{/fringe}$$

the fringe order found at the top and bottom of the circular hole of figure 11 on page 31 was $n = 3.75$. The stress at these points were calculated to be:

$$\sigma_1 - \sigma_2 = nF$$

$$\sigma_1 - \sigma_2 = (3.75)(2.55) = 9.56 \text{ lb/in}^2$$

the applied stress S was equal to 9.22 psi the percentage difference found by comparing the theoretical stress to actual stress

$$\frac{9.56 - 9.22}{9.22} \times 100 = 3.7\%$$

The theoretical stress concentration factor at the sides of a circular hole in a semi-infinite plate is given as 3. The S.C.F. found at the side points A and B by the test was

$$\sigma_A = 9.75\ (2.55) = 24.8 \text{ lb/in}^2$$

$$\sigma_B = 9.75\ (2.55) = 24.8 \text{ lb/in}^2$$

the S.C.F. is found by dividing the stress at points a and b by the applied stress

$$S.C.F. = \frac{24.8}{9.22} = 2.7$$

Since the model was not an infinite plate, the S.C.F. decreases accordingly. Figure 12 on page 34 shows the theoretical effect of the finite dimension on the S.C.F. at the hole (32). For the ratio of hole diameter to width of the sheet of 1.46, the theoretical S.C.F. from figure 12 was determined as 2.47.

This gives a percentage deviation of:

$$\frac{2.7 - 2.47}{2.47} \times 100 = 9.4\%$$

Another check was performed on a circular hole in a semi-infinite homogeneous medium. In this test, the ratio of the hole diameter to the total width of the sheet was changed to 0.97, all other dimensions and loads were duplications of the first test. The results of this test are given in table 2 on page 41.

FIGURE NO. 12

Graph of Stress Concentration Factor vs. d/D Ratio

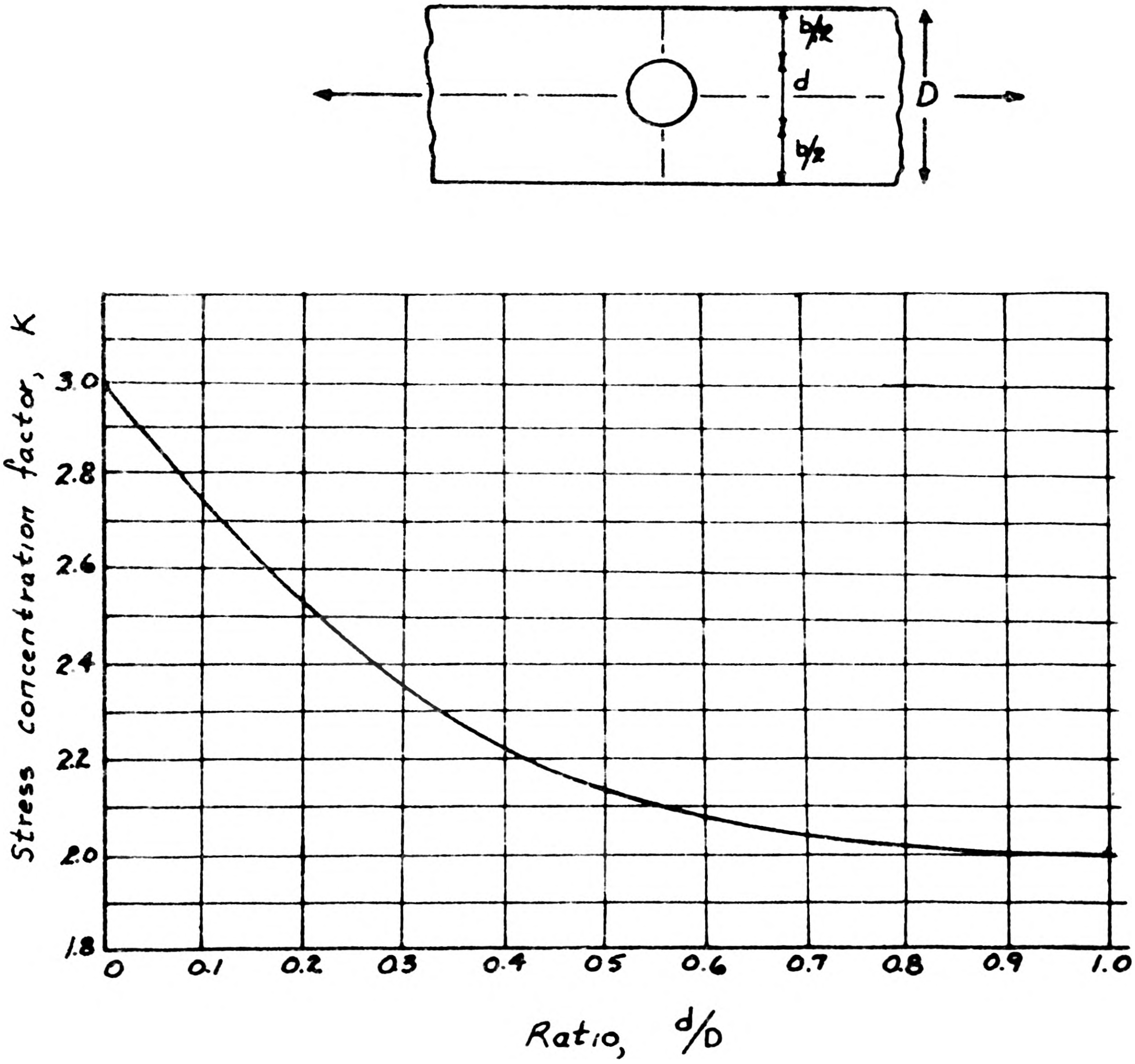

TEST OF A CIRCULAR OPENING IN A TWO LAYERED MEDIUM MODEL PREPARATION

Model Preparation

The specific test run in this study consisted of a circular hole in a two layered medium. The hole was placed as shown in figure 13 on page 38. Both layers consisted of cured epoxy resin and each was considered homogeneous. One layer was cast in the molding device and allowed to cure. After curing, the top of the sheet was machined to a smooth flat surface. The mold was reassembled with clamps on the Lucite sheets to prevent leakage of the liquid epoxy of the second layer onto the first solidified layer. The second layer was poured directly on the first layer and allowed to solidify. The two layers differed only in their chemical compositions such that after curing, the layers would have different physical characteristics. In this test case, the two layers differed in their modulus of Elasticity by a factor of approximately 2.

Calibration

Both layers were calibrated for their material fringe value just before testing. The procedure was the same as previously stated in the section on calibration. Layer one, top layer of figure 13 on page 38 , had a material fringe value of $f = 1.335$ lb/in/fringe, and a model fringe value of 2.74 lb/in^2/fringe. Layer two had a material fringe value of 1.09 lb/in^2/fringe and a model fringe value of 2.22 lb/in^2. The modulus of elasticity for each of the two materials was also measured, immediately after testing. A beam was cut from each layer and used for the measurement of the Modulus of elasticity as previously outlined. The values obtained were $E = 120$ lb/in^2 for the bottom layer and $E = 300$ lb/in^2 for the top layer.

Results of Two Layer Test

Figure 13 on page 38 shows the fringe distribution obtained from the two layer test. The stress at the top and bottom of the hole are as follows:

$$\sigma_{top} = 2(2.74) - 5.48 \text{ psi}$$

$$\sigma_{bottom} = 2.5(2.72) = 5.50 \text{ psi}$$

This compares with the theoretical stress at the top and bottom of a hole in a homogeneous material which was found to be:

$$\sigma = 5.46 \text{ psi}$$

The stress at the sides of the circular hole in the two layer case was calculated at two places. One just above the boundry and one just below the boundry as indicated in figure 14 on page 41. These values were calculated to be:

$$\sigma_A1 = 7.5\ (2.74) = 20.5 \text{ psi}$$

$$\sigma_B1 = 8\ (2.22) = 17.8 \text{ psi}$$

The theoretical value for the stress at a point in a homogeneous medium exactly on the side of the circular hole point A was calculated to be:

$$3\sigma = 3\ (5.46) = 16.38 \text{ psi}$$

The S.C.F. for point A^1 is

$$(S.C.F.)_{A^1} = \frac{20.5}{5.46} = 3.75$$

and for point B is

$$(S.C.F.)_{B^1} = \frac{17.8}{5.46} = 3.25$$

Figure 13

Fringe Distribution Around a Circular Hole in a Two Layered Medium

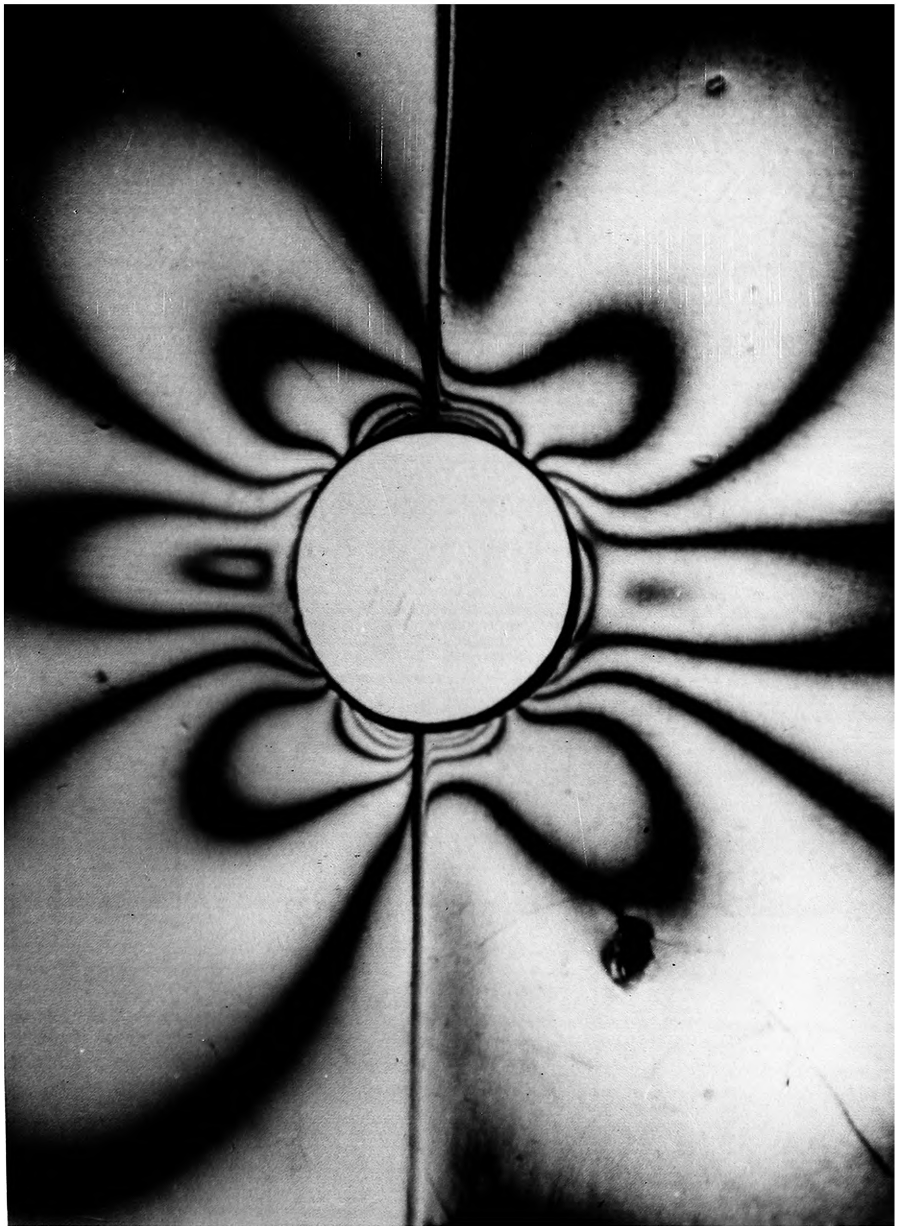

DISCUSSION OF RESULTS

The experimental results found for the S.C.F. at critical points around a circular opening in a homogeneous medium were consistently higher than the theoretical. Therefore, the values found for the S.C.F. in the two layer case would have to be considered as being somewhat higher than the theoretical. However, the magnitude of increase in the S.C.F. in the two layer case compared to the increase of the S.C.F. in the homogeneous case was much higher than could be attributed to errors in the loading and calibration procedures. Therefore, the effect of the different moduli of elasticity in a two layer would increase the S.C.F. around a circular opening, the magnitude depending on the difference between the moduli of elasticity of the two quantities and their respective Poisson's ratio. A large difference of the moduli of elasticity for the material would increase the effect of elastic constraint and the S.C.F. factor, provided Poisson's ratio for the respective materials were approximately the same. In this study, Poisson's ratio for each material was approximately the same.

If this two layer test was applied to a mine prototype, that is, an opening between two layers with different moduli of elasticity, the sequence of loading must be considered in comparison with the sequence in the model construction. Since the layers in the earth were deposited over long periods of time, the shearing stress or elastic constraint, at the boundry between the layers could either have been increased by tectonic forces or decreased due to creep or faults. If the shearing stress between the two layers was decreased due to creep, the model should not have shear stresses at the boundry between the layers under load. However, the model was constructed in such a manner that there existed a shear stress at the boundry under load. When an opening is placed in this model, an additional increase in S.C.F. probably causes the S.C.F. to be higher than the mine prototype.

The stress distribution about openings which occur between two layers of brittle materials such as limestone and sandstone, is especially susceptible to high stress concentrations. If the boundry located near points of greatest tensile stress the danger of cracking and spalling of the material would be greatly increased due to the added effect of elastic constraint on the S.C.F.

CONCLUSIONS

Table 2 on page 41 summarizes the results obtained from the one layer and two layer tests. This table indicates the effect of elastic constraint on the boundry of the layered medium increases the stress concentration factor from that obtained from test on circular openings in a homogeneous medium. This change is greatest very close to the boundry and becomes negligible a short distance from the boundry. This is shown by the very close agreement between theoretical and experimental values at the top and bottom of the hole a relatively great distance from the boundry.

Since the stress concentration factor is a very important quantity in any brittle material, the fact that it increases close to the boundry would indicate a careful choice of openings should be made. Any position for the opening close to the point of its greatest stress concentration would only increase the stress concentration factor. Hence, this would increase the danger for cracking or spalling in the material.

In the case of a circular opening in a two layered medium, the opening should not be placed with its horizontal diameter coinciding with the boundry. Any other position would not increase the stress concentration factor above the critical one which is along the horizontal diameter of the hole.

If these results are applied directly to a mine stress problem, a possible source of discrepency could come from the fact that because the beds of the earth are layed down over long periods of time the shear stresses along the boundry of the two layers is probably dissipated. Therefore, the stress concentration factor at the hole would be decreased from the case where the load is applied directly to layers which were cured in an unstressed state.

The close agreement between theoretical and experimental values obtained in this study, indicate that, cured epoxy resin material can be effectively used as a photoelastic material. Since this material can easily be case into layers with dissimilar moduli of elasticity, the actual condition in the earth could be more closely approximated. Also, it has been shown possible to analyze the stress around openings close to the boundry of two metals with different physical properties.

FIGURE NO. 14

Location of Points for which the S.C.F. was Determined

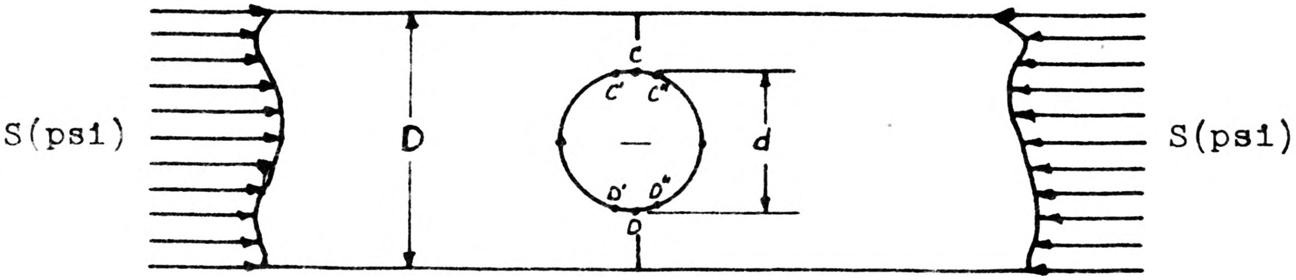

TABLE NO. 2

Results of S.C.F. at Critical Points

TEST	POINT	THEORETICAL S.C.F.	EXPERIMENTAL S.C.F.
homogeneous (1)	A,B	.9	1.05
d/D = .146	C,D	2.47	2.70
homogeneous (2)	A,B	.96	1.02
d/D =.097	C,D	2.80	3.00
Two layer	C',D'		3.75
d/D = .135	C",D"		3.25
	A		1.00
	B		1.00

SELECTED REFERENCES

1. BOUSSINESQ, J., 1885, "Applications des Potentials", Paris, France.

2. FLAMANT, 1892, Compt. Rend., Vol. 114, page 1465.

3. MICHELL, J.H., 1902, Proceedings London Mathematics Society, Vol. 34, page 134.

4. TIMOSHENKO and GOODIER, 1951, Theory of Elasticity, McGraw-Hill, New York, New York.

5. COKER and FILON, 1957, Photoelasticity, 2nd Ed., Cambridge Press.

6. BUCKEY and SINCLAIR, 1940, "Photoelasticity and its Application to Mine-pillar and Tunnel Problems", AIME Trans.

7. PANEK, L.A., 1951, Stresses About Mine Openings in a Homogeneous Rock Body, Edward Brothers, Ann Arbor, Michigan.

8. DUVALL, WILBUR I., 1948, "Stress Analysis Applied to Underground Mining Problem", U. S. Bureau of Mines Reports, 4192, 4387.

9. VAN POOLLEN, H.K., 1956, "Horizontal Supports of Mine Openings", Colorado School of Mines, Vol. 51.

10. MOYE, D.G., 1958, "Rock Mechanics in the Investigation and Construction of T. No. 1 Underground Power Station, Snowy Mts., Australia", Annual Meeting G.S.A., St. Louis, Missouri, November 6-8.

11. POTTS, E.L., 1954, "Stress Distribution, Rock Pressures and Support Loads", Colliery Eng.

12. DIXON, J., 1954, "Stress Distribution in Auger Mining and WhenWorking Seams in Close Proximity", U. of Durham, Research Publication, Vol. 2, pp. 41-47.

13. ROUX, A.J., DINKHAUS, H.G., and LEEMAN, E.R., 1957, "Stresses in and the Condition of the Ground Around Mining Excavations", Canadian Mining and Metallurgy Bull.

14. JUDD, W.R., 1958, "Effect of Elastic Properties of Rocks on Civil Engineering Design", Annual Meeting Geo. Soc. of America, St. Louis, Mo., Nov. 6-8.

15. PHILLIPPE, R.R., and MELLINGER, F.M., 1957, "Theoretical and Experimental Stress Analysis", Quarterly of Colorado School of Mines, Vol. 52, No. 3.

16. PHILLIPPE. R.R. and MELLINGER F.M., 1948, "A Study of Photoelastic Models of Foundations", Proc. Sec. Ann. Inter. Conf. on Soil Mechanics, Vol. 5, p. 58.

17. KNAPPEN and PHILLIPPE, R.R., 1936, "Resisting Strength of Foundations", Practical Soil Mechanics at Muskingam, Part III, Eng. News Record, April 23.

18. CORPS OF ENGINEERS, 1957, Report of Comparative Photoelastic Study of Stresses in Foundations of Flood Walls with Sloping and Horizontal Bases, August.

19. TAN, EK-KHOO, 1943, "Stability of Soil Slopes", ASCE proc., Vol. 73, p. 19.

20. FARQUHARSON, F.B., and HENNES, R.G., 1940, "Gelatin Models for Photoelastic Analysis in Earth Masses", Civil Eng., Vol. 10.

21. CORPS OF ENGINEERS, 1951, "Report of Initial Comparative Photoelastic Study of Rigid Versus Flexible Culverts", Ohio River Div. Labs, Mariemont, Ohio.

22. CUYKENDALL, T.R., 1940, "Gelatin Photoelastic Models", The Cornell Engineer, December 1940, pp. 9-13.

23. CRISP, J.D., 1953, "The Use of Gelatin Models in Structural Analysis", Institute of Mechanical Engineering.

24. MYLONAS, C., 1955, "Experiments with Composite Models", SESA, Vol. XII, No. 2, pp. 129-142.

25. SPOONER, H., and McCONNELL, L.C., 1953, "An Ethozylene Resin for Photoelastic Work", British Journal of Applied Physics, Vol. 4, pp. 181-184.

26. AGOSTINO, J.D., DRUCKER, D.C., LIU, C.K., and MYLONAS, C., 1955, SESA, Vol. XII, No. 2, pp. 123-128.

27. DURELLI, A.J., and RILEY, W.F., 1958, "Experiments for the Determination of Transient Stress and Strain Distributions in Two-Dimensional Problems", Journal of Applied Mechanics, Paper No. 56-A-11.

28. RILEY, W.F., DALLY, J.W., and DURELLI, A.J., 1958, Journal of Applied Mechanics, Vol. 25, No. 2, pp. 189-195.

29. LEE, HENRY and NEVILLE, KRIS, 1957, Epoxy Resins, McGraw-Hill Book Company, New York, New York, pp. 1-6.

30. CIBA TECHNICAL DATA BULLETIN NO. 4, "Araldite 502", Ciba Chemical Corporation, Fairlawn, New Jersey.

31. FROCHT, M.M., 1957, Photoelasticity, Vol. 1, John Wiley and Sons, Inc., pp. 2-32.

32. HEYWOOD, R.B., 1952, Designing by Photoelasticity, Chapman and Hall Ltd., London, England, p. 268.

VITA

Donald Frank Haber was born November 8, 1933, at St. Louis, Missouri. He received elementary and high school education in St. Louis, Missouri.

He enrolled in the School of Mines and Metallurgy, University of Missouri, Rolla, Missouri, in 1951, and received a Bachelor of Science Degree in Mining Engineering in June 1956. In 1958 he was appointed an Instructor in the Mechanics Department at the Missouri School of Mines and Metallurgy and was enrolled as a graduate student in Mining Engineering.

In February of 1962 he received his Registered Engineering license from the State of Missouri.

He has been employed by the U. S. Bureau of Mines, Mining Research Branch at Rolla during 1959 thru 1962.